

Anodic Behaviour of Some Bispyridinium Oximes on a Glassy-Carbon Electrode

Ivana Novak^{1,*}, Šebojka Komorsky-Lovrić², Suzana Žunec¹, Ana Lucić Vrdoljak¹

¹ Institute for Medical Research and Occupational Health, Ksaverska Cesta 2, HR-10000 Zagreb, Croatia

² “Ruđer Bošković” Institute, Bijenička 54, HR-10000 Zagreb, Croatia

*E-mail: inovak@imi.hr

Received: 2 May 2013 / Accepted: 10 June 2013 / Published: 1 July 2013

The electrochemical oxidation of selected bispyridinium oximes, including conventional oximes HI-6 [(1-(((4-carbamoylpyridinium-1-yl)methoxy)methyl)-2-((hydroxyimino)-methyl)pyridinium chloride] and TMB-4 [*N,N'*-(propano)bis(4-hydroxyiminomethyl)pyridinium bromide], as well as a new generation oxime K048 [1-(4-hydroxyiminomethylpyridinium)-4-(4-carbamoylpyridinium) butane dibromide], was studied at a glassy-carbon electrode over a wide range of experimental conditions, using cyclic and square-wave voltammetry. It was observed that in all investigated compounds the oxidation of oxime moiety (the first oxidation peak) occurs. This process is diffusion controlled, pH dependent, and occurs in a complex ECE mechanism. The monoximes HI-6 and K048 exhibited only one anodic peak, while TMB-4 undergoes two consecutive oxidation reactions due to the presence of two oxidizable oxime moieties. The final product of electro-oxidation of oxime moiety, hydroxy-nitroso intermediate, undergoes further oxidation at more positive potential.

Keywords: bispyridinium oximes, HI-6, K048, TMB-4, cyclic voltammetry, square-wave voltammetry, electrochemical oxidation

1. INTRODUCTION

Oximes have been extensively investigated over the past decades as a pharmacologically active compounds with a great potential in the treatment of organophosphorus (OP) pesticides and nerve agents poisoning [1,2]. The primary mechanism of action of oximes as antidotes is to reactivate acetylcholinesterase (AChE) inhibited by OP compounds [3]. Reactivation proceeds as a two-step reaction via formation of an intermediate Michaelis Menten complex based on displacing the OP phosphoryl moiety from the AChE active site serine by virtue of oxime's high affinity for the enzyme,

powerful nucleophilicity and physiologically compatible pK_a [4]. Among the many classes of oximes investigated so far, those that found clinical application can be divided into the monopyridinium (pralidoxime, 2-PAM) and bispyridinium (trimedoxime, TMB-4; obidoxime, LüH-6; and asoxime, HI-6) ones [5]. However, none of these oximes is sufficiently effective against all of the known OP compounds. Within the last few years, a new generation of so-called K-oximes was developed in the Czech Republic [6] by modifying the structure of the four above mentioned conventional oximes. Promising results using several of K-oximes were obtained for poisoning by the OP nerve agent tabun [7-9] as well as in the case of OP pesticides poisoning [10,11]. Despite convincing evidence of their pharmacological effects, questions about their alternative bioactivities are still incomplete. Recently, studies indicating an antioxidant activity of some oxime derivatives were published [12-15]. As reported, antioxidative potential of oxime molecule could be due to its scavenging activity toward different forms of reactive species like hydroxyl radicals, nitric oxide radicals, and hydrogen peroxide, and also related with its metal chelating properties [14]. Concerning pyridinium oximes, incorporated iminium and oxime moieties are electron-affinic which enables them various physiological properties [16]. In 2007 our group reported for the first time results concerning potential antioxidant activity of the conventional oxime HI-6 *in vitro* [17]. Later on, several *in vivo* studies showed involvement of pyridinium oximes in a processes including antioxidant power balance [18-20]. It is known that large number of biologically active compounds or their metabolites exhibit reduction potentials greater than -0.5 V which can permit electron acceptance from *in vivo* donors [21].

The investigation of the redox behaviour of pyridinium oximes using electrochemical techniques could provide valuable insights into the biologically relevant redox reactions of this class of compounds. The electro-reduction of mono- and bis- pyridinium oximes has been considered to be a reasonably well understood area of organic electrochemistry [22-24]. However, the literature data on the mechanisms of electrochemical oxidation of pyridinium oximes is extremely scarce. To the best of our knowledge, there is one published study concerning the electro-oxidation behaviour of monopyridinium oxime pyridine-2-aldoxime methochloride (PAM chloride) at poly(*p*-toluene sulfonic acid) modified glassy-carbon electrode [25], but no data are available on the anodic behaviour of bispyridinium oximes.

The present study is concerned with the investigation of the electrochemical oxidation mechanisms of selected bispyridinium oximes (HI-6, TMB-4 and K048) using cyclic (CV) and square-wave voltammetry (SWV) at a glassy-carbon electrode (GCE). The investigation of the electro-oxidation mechanisms of bispyridinium oximes is important since it provides results that are relevant for better understanding of their biological redox reactions and their physiological mechanism of action in general.

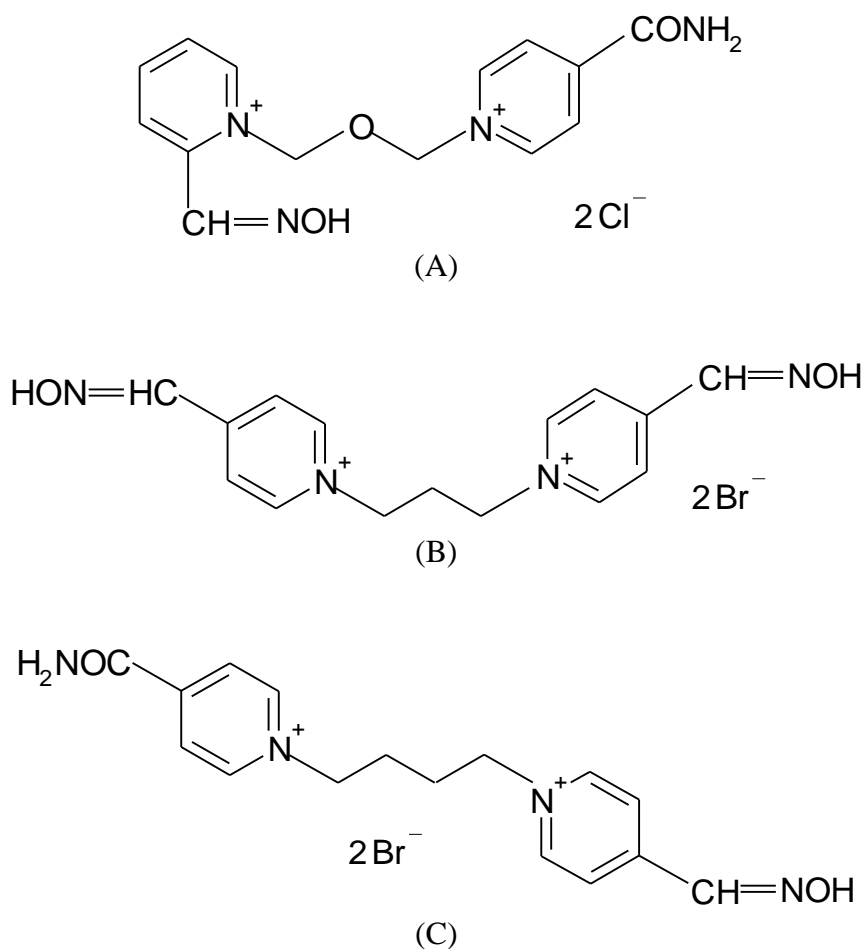
2. EXPERIMENTAL

2.1 Reagents

HI-6 was synthesized at the University of Defence Hradec Kralove, Czech Republic. TMB-4 was obtained from Bosnalijek, Sarajevo, Bosnia and Herzegovina. K048 was synthesized at the

Department of Toxicology, Faculty of Military Health Sciences, Hradec Králové, Czech Republic. Chemical structures of investigated oximes are shown in Scheme 1.

Stock standard solutions of oximes ($c = 2 \times 10^{-2}$ M) were prepared from the dry pure substances in deionized water obtained from Millipore Milli-Q purification system (resistivity ≥ 18 M Ω cm). The stock solutions were protected from light and kept in a refrigerator. All buffer solutions (pH 3-11) were from Kemika, Zagreb, Croatia, analytical grade. For the supporting electrolyte analytical grade KNO₃ (Kemika, Zagreb, Croatia) was used.



Scheme 1. Chemical structures of HI-6 (A), TMB-4 (B) and K048 (C).

2.2 Instrumentation

All voltammetric measurements were carried out using the computer-controlled electrochemical system Autolab PGSTAT 30 (Eco-Chemie, Utrecht, Netherlands). Voltammetric curves were recorded using a three-electrode system (Metrohm, Switzerland) with glassy-carbon electrode of 3.0 mm diameter (MF-2012, Bioanalytical Systems, Inc., West Lafayette, Indiana, USA) as a working electrode, Ag/AgCl (3 M KCl) electrode as a reference electrode and platinum wire as a counter electrode. Before each run the glassy-carbon electrode was polished with diamond spray (6 μ m), and rinsed with ethanol and deionized water. The solutions were degassed with high-purity nitrogen

prior to the electrochemical measurements. A nitrogen blanket was maintained thereafter. All experiments were performed at room temperature.

3. RESULTS AND DISCUSSIONS

3.1 HI-6

Fig. 1 shows cyclic voltammograms of 2×10^{-3} M HI-6 solution at two different scan rates. At scan rate (ν) of 10 mV s^{-1} , the first scan (Fig. 1A, black curve) consists of two anodic peaks, peak 1 at 0.690 V, and peak 2 at 1.162 V. On scanning in the negative direction, no reduction peaks were observed, indicating that oxidation of HI-6 is an irreversible process. By increasing the scan rate, the second anodic peak diminishes and finally disappears at $\nu \geq 100 \text{ mV s}^{-1}$ (see Fig. 1B).

Successive cyclic voltammograms recorded in the potential range from 0.250 V to 1.250 V without polishing the electrode surface between the measurements are shown in Fig. 1A. As can be seen, in the second scan peak 1 splits and a new peak appears at 0.827 V, while the potentials of the peaks appearing in the first scan shift to more positive values and their peak currents decrease. In the third and subsequent scans anodic current of new peak 3 increases, while the former first and second peaks are diminished further. In order to check the origin of peak 3, a new CV experiment was carried out but the scan direction was reversed at 1.020 V, after the occurrence of peak 1 and before peak 2 (data not shown). Again, peak 3 occurred on a second and subsequent scans showing that this peak could be due to oxidation of intermediates formed during the first electrode reaction. We assume that the HI-6 oxidation intermediates adsorb on the electrode surface. Consequently, anodic current of peak 3 increases on the subsequent scans, and the peak potential is shifted in the positive direction since higher energy is needed for the redox reaction which proceeds from the adsorbed state [26, 27]. On the other hand, adsorbed layer blocks the electron transfer between dissolved reactant and electrode surface leading to significant decrease in peak 1 and peak 2 currents and to the shift of their potentials toward more positive values.

The effect of scan rate on the current and potential of peak 1 was also investigated. Cyclic voltammograms were recorded for $10 \leq \nu \leq 500 \text{ mV s}^{-1}$ in pH 9 buffer containing 2×10^{-3} M HI-6 always using a freshly polished electrode surface. The influence of the square root of scan rate ($\nu^{1/2}$) on the peak 1 current showed a linear relationship within the whole range studied, which is typical for a diffusion controlled oxidation process of a solution species. The peak 1 potential varies linearly with the logarithm of the scan rate changing by 27 mV per decade, which confirms the irreversible nature of oxidation process. From the relationship ΔE vs. $\Delta \log \nu$ the product $\alpha n = 1.08$ was calculated, where α is the transfer coefficient and n is the number of electrons involved.

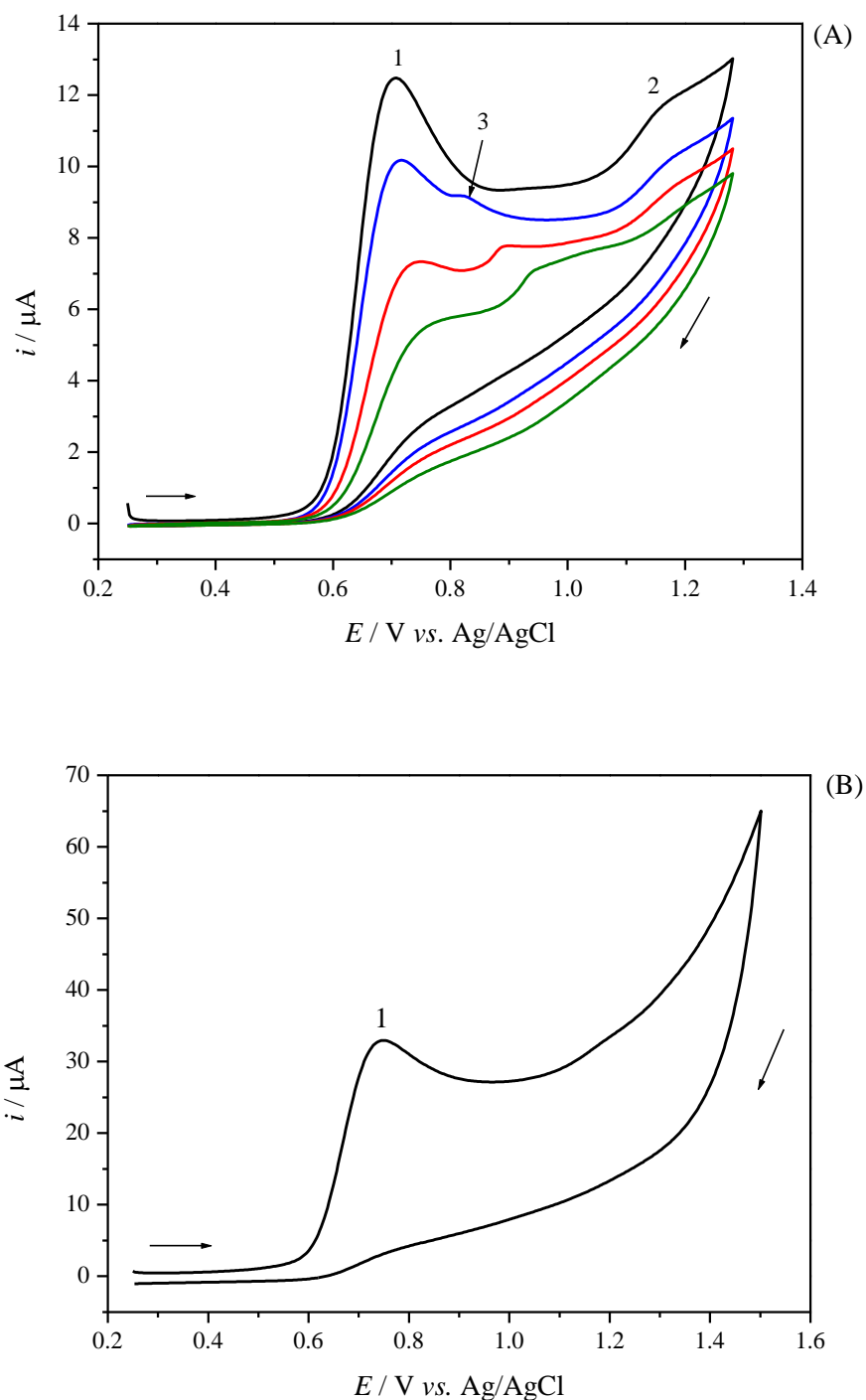


Figure 1. Cyclic voltammograms of $2 \times 10^{-3} \text{ M}$ HI-6 in 0.1 M KNO_3 at pH 9: for (A) $\nu = 10 \text{ mV s}^{-1}$, (black curve) 1st, (blue curve) 2nd, (red curve) 3rd and (green curve) 5th scan, and (B) $\nu = 100 \text{ mV s}^{-1}$, 1st scan. The potential increment is 3 mV.

Square-wave voltammograms recorded at different frequencies in $1 \times 10^{-3} \text{ M}$ solution of HI-6 in pH 7 buffer showed similar features to the cyclic voltammograms. At low frequencies, the net SW response consists of a predominant peak at 0.700 V, and a broad and ill-defined wave at about 1.100 V, which completely disappears at frequencies above 25 Hz (Fig. 2). The net peak potential of peak 1 is a

linear function of the logarithm of frequency (for $10 \text{ Hz} \leq f \leq 500 \text{ Hz}$) with the slope of $\Delta E_{p,1}/\Delta \log f = 32 \text{ mV/d.u.}$ that corresponds to $\alpha n = 0.91$, which is nearly the same value as that obtained by cyclic voltammetry.

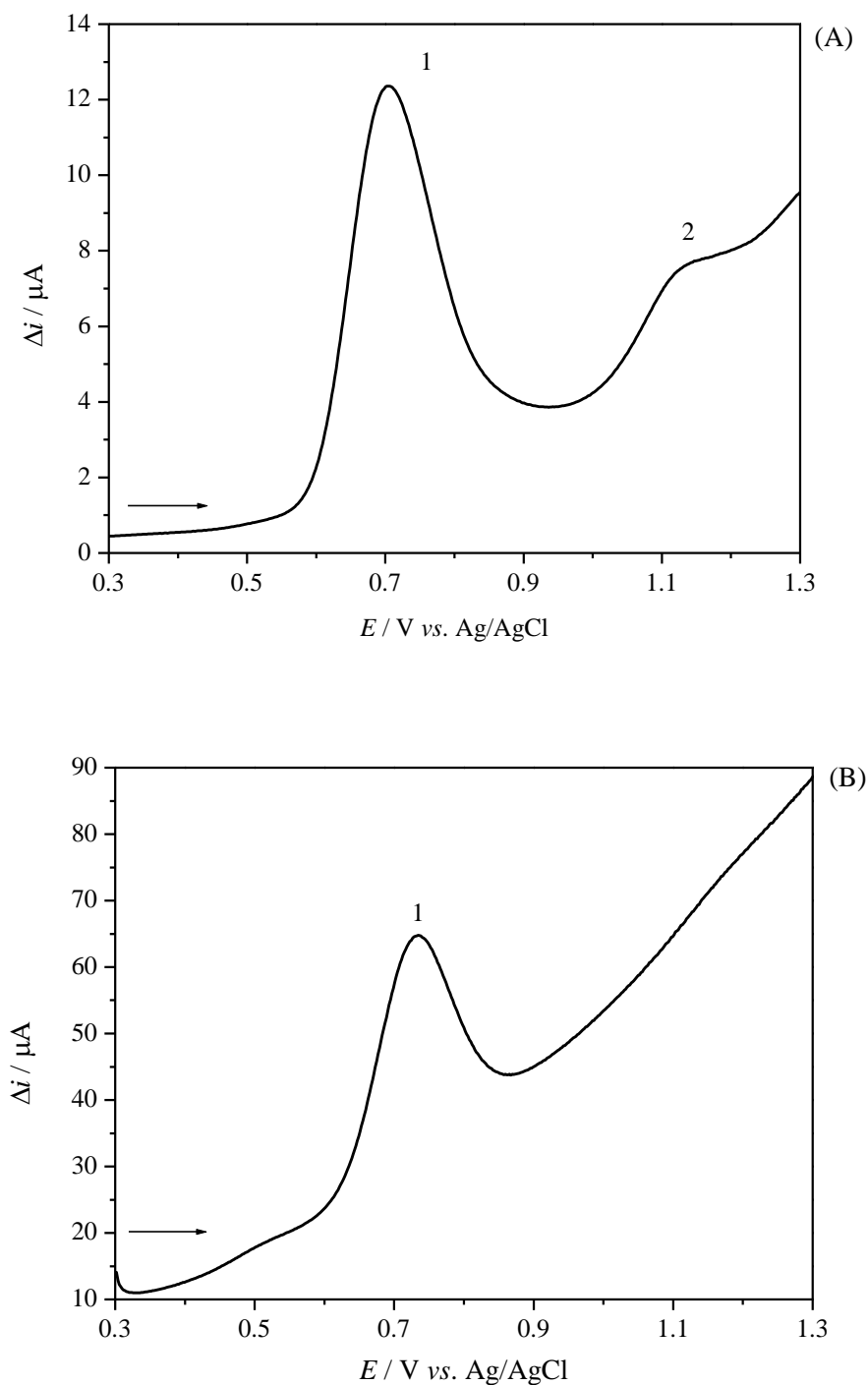


Figure 2. The net square-wave voltammetric responses of $1 \times 10^{-3} \text{ M HI-6}$ in 0.1 M KNO_3 at pH 7 for: (A) $f = 8 \text{ Hz}$, and (B) $f = 100 \text{ Hz}$. The amplitude is 50 mV and the potential increment is 2 mV.

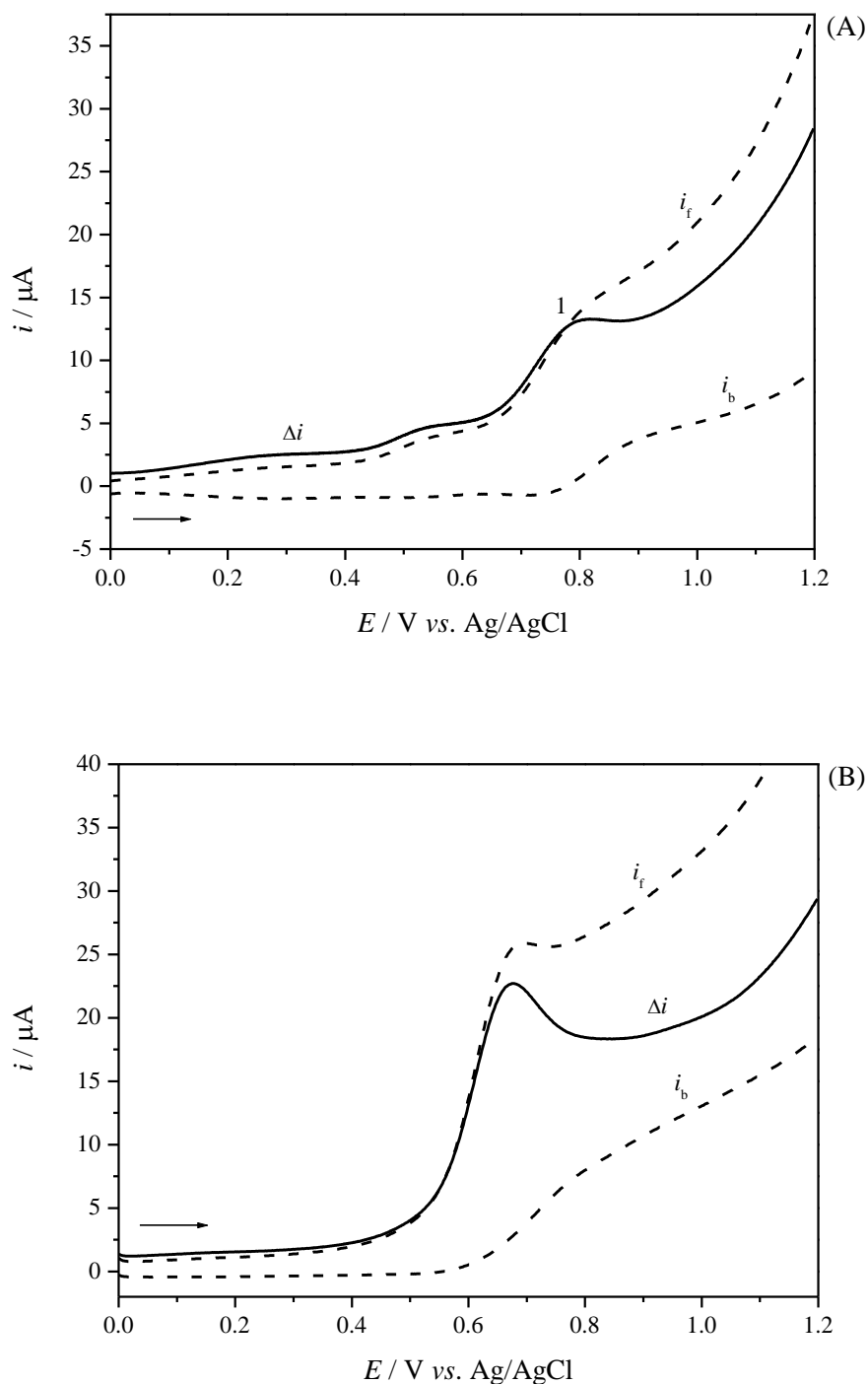


Figure 3. Square-wave voltammograms of 5×10^{-4} M HI-6 in 0.1 M KNO_3 at: (A) pH 6 and (B) pH 11. The net response (Δi) and its forward (i_f) and backward (i_b) components are shown. The frequency is 100 Hz, the amplitude is 50 mV and the potential increment is 2 mV.

The influence of pH on electrochemical oxidation of HI-6 was studied using square-wave voltammetry at a frequency of 100 Hz over a wide pH range between 3 and 11. The SW responses were all recorded in 5×10^{-4} M solutions of HI-6 in different buffers containing 0.1 M KNO_3 as the

supporting electrolyte. No oxidation peak for HI-6 was observed below pH 6. In a pH range between 6 and 11, HI-6 exhibited one well defined oxidation peak. If $6 \leq \text{pH} \leq 8$, SW responses of HI-6 contain both forward (oxidative) and backward (reductive) components, implying a reversible or quasireversible electrode oxidation (Fig. 3A). By increasing pH above pH 8, the reductive peak vanishes indicating irreversible electron transfer process (Fig. 3B). The effect of pH on the current and potential of peak 1 is shown in Fig. 4. The net peak potential was displaced to less positive values by increasing pH. The dependence was linear over the pH range between 6 and 10 according to the equation: $E_p = 0.948 - 0.029 \text{ pH}$. The slope of ca. 30 mV per pH unit suggested that the mechanism of electrooxidation of HI-6 involves a number of electrons that is double the number of protons. Above pH 10 the net peak potential is pH independent, indicating that hydrogen ions were no longer concerned with the electrode reaction. The net peak current increases with pH, reaching a maximum at pH 9.

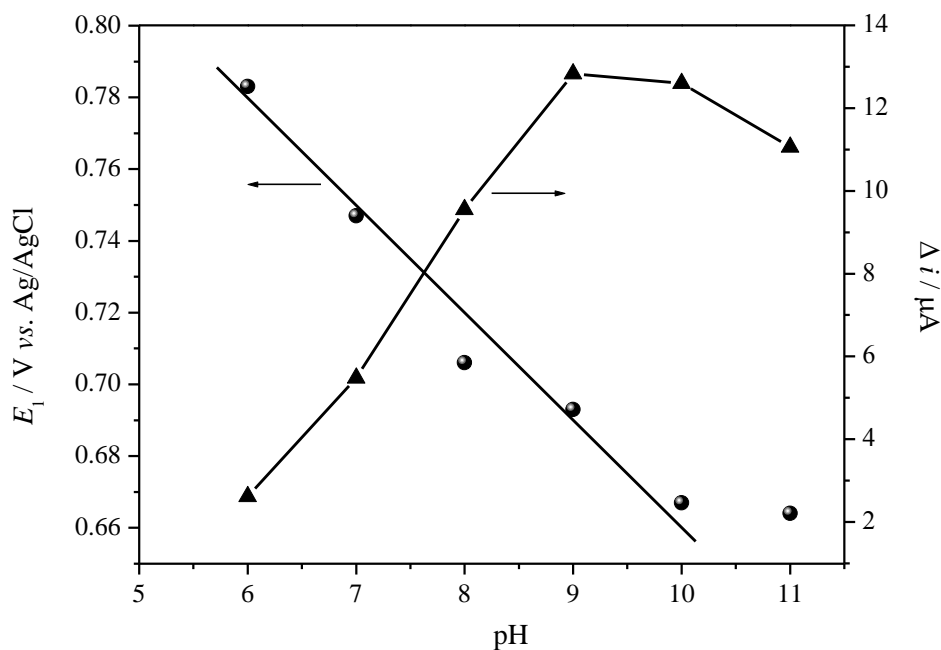
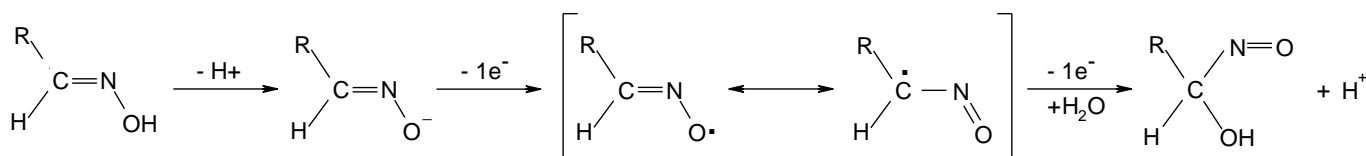


Figure 4. Dependence of net peak potentials (●) and net peak currents (▲) of the first electrode reaction of HI-6 on pH of electrolyte. All other data are as in Fig. 3.

The electroactive centres in HI-6 molecule are *ortho*-positioned oxime group and *para*-positioned primary amide group. Primary amides cannot be oxidized at potentials lower than 2 V vs. SCE [28], which is out of the potential range of the glassy-carbon electrode in aqueous solutions. Considering that, it could be concluded that peak 1 corresponds to oxidation of oxime moiety. According to the literature data [25, 29] the electrochemical oxidation of oxime moiety proceeds via two successive monoelectronic steps. Since the voltammetric response of HI-6 can be obtained only at pH close to the pK_a of the oxime group (for pK_a values see reference [30]), we assumed that spontaneous and fast deprotonation precedes the electron transfer reaction, meaning that, in this first step, deprotonation is not the rate determining step and protons are not involved in redox equilibria.

So, the first step of the electrochemical oxidation of HI-6 involves a single-electron abstraction from the anion oxime group, leading to the formation of iminoxy radical. Our results indicate that the stability of iminoxy radical depends significantly on the pH value. This is in accordance with Kim et al. [31], who claimed that the lifetime of electrophilic iminoxy radical is strongly affected by the nucleophilic attack by hydroxide ions. At $\text{pH} > 8$, iminoxy radical is very unstable and immediately reacts with hydroxide ions from the solvent in a subsequent chemical reaction. So, the follow-up chemical reaction (i.e. the nucleophilic attack by water) consumes a significant amount of iminoxy radical and the backward component of the response vanishes. On the other hand, by decreasing pH, the reversibility of the reaction increases indicating longer lifetime of iminoxy radical. Namely, at lower pH the rate of chemical transformation is diminished due to lower concentration of hydroxide ions, and the backward component of the response is developed indicating apparently reversible electrode reaction. The second electrochemical oxidation step involves a single-electron abstraction and formation of hydroxy-nitroso intermediate. The mechanism of electrochemical oxidation of oxime moiety is shown in Scheme 2. In conclusion, the first anodic peak of HI-6 corresponds to the oxidation of anion oxime moiety to hydroxy-nitroso intermediate, which follows the above described ECE mechanism. The origin of the second oxidation wave is at the moment not clear. However, we assume that this peak might be due to the oxidation of hydroxyl group in hydroxy-nitroso intermediate to produce carbonyl compound. Assumingly, this electrode reaction is too slow and redox peak can be observed only at very low scan rates.



Scheme 2. Proposed mechanism for the electrochemical oxidation of oxime moiety.

3.2 K048

Fig. 5 shows cyclic voltammograms (a few successive scans) of 5×10^{-4} M solution of K048 recorded at pH 9 and scan rate of 10 mV s^{-1} . On the first CV scan, K048 showed the occurrence of two consecutive anodic processes, main and well-defined peak 1 at $E_1 = 0.636 \text{ V}$, and a broad and ill-defined peak 2 at $E_2 = 1.00 \text{ V}$. Changing the scan direction, no cathodic peaks appeared. On the second CV recorded in the same conditions without cleaning the electrode surface, peak 1 splits and a new anodic peak 3, at $E_3 = 0.741 \text{ V}$, occurred. At the same time, the currents of peaks 1 and 2 decreased due to the adsorption of K048 and/or oxidation products at the GCE surface.

The effect of scan rate on anodic peaks of K048 was evaluated at pH 9 in the range between 10 mV s^{-1} and 500 mV s^{-1} . By increasing the scan rate the potential of peak 1 remained almost constant. Peak 1 current was directly proportional to the square root of scan rate indicating that K048 oxidation is a diffusion controlled process. Peak 2 disappeared at $v \geq 100 \text{ mV s}^{-1}$.

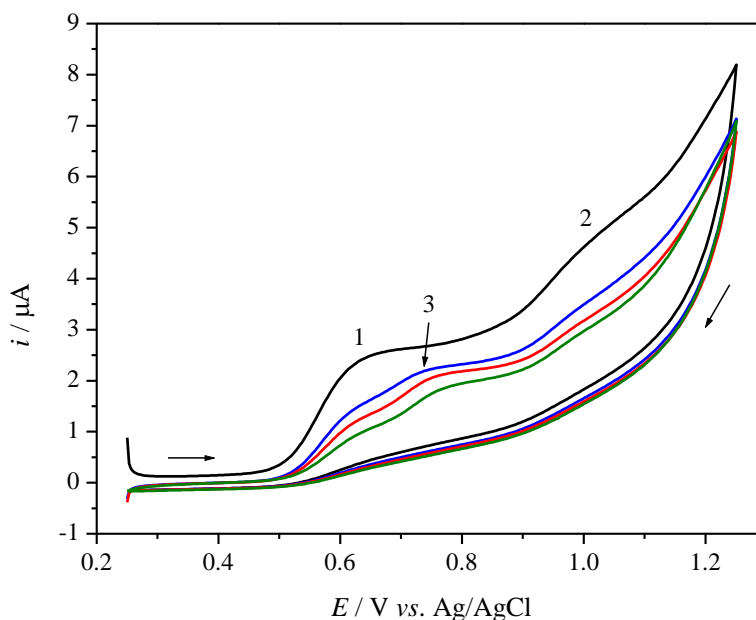


Figure 5. Successive cyclic voltammograms of 5×10^{-4} M K048 in 0.1 M KNO_3 at pH 9: 1st (black curve), 2nd (blue curve), 4th (red curve) and 7th (green curve) scan. Scan rate is 10 mV s^{-1} and the potential increment is 3 mV.

Square-wave voltammograms were performed at different frequencies ($8 \text{ Hz} \leq f \leq 500 \text{ Hz}$) in 5×10^{-4} M K048, at pH 9. K048 yielded one well-defined and sharp peak 1, and one broad and ill-defined wave (named here as peak 2), see Fig. 6. If $f = 8 \text{ Hz}$ and $\text{pH} = 9$, peaks 1 and 2 appear at 0.580 V and 0.980 V, respectively. By increasing the frequency the potentials of both peaks were slightly shifted toward more positive values. The net peak currents increased proportionally with an increase of frequency up to 100 Hz. Moreover, peak 2 current was directly proportional to the frequency, characterizing an adsorption controlled processes. The backward component of the first SW response of K048 is poorly pronounced at frequencies above 50 Hz and completely disappears at lower frequencies. Such voltammetric behaviour could be explained by EC mechanism in which quasireversible electrode reaction is followed by the irreversible chemical reaction [32]. Above frequency of 250 Hz, an ill-defined SW response was obtained, probably due to excessive effect of IR-drop.

The pH dependence has analogous trend as for HI-6 (data not shown). In the acidic electrolyte ($\text{pH} < 7$) no response can be recorded. In the range between pH 7 and pH 10 the potential of peak 1 is approximately a linear function of pH, with the slope -31 mV/d.u. Above pH 10 the potential of peak 1 is independent of pH. Peak 1 current reached a maximum at pH 10. Potential of peak 2 was independent of pH in the whole range.

The obtained results indicate that electro-oxidation of K048 follows a mechanistic pathway analogous to that proposed for HI-6, which involves oxidation of anion oxime group to hydroxynitroso intermediate via two-electrons one-proton ECE mechanism (see Scheme 2). The product of the first electrode reaction of K048 adsorbs on the electrode surface and undergoes further oxidation at more positive potential.

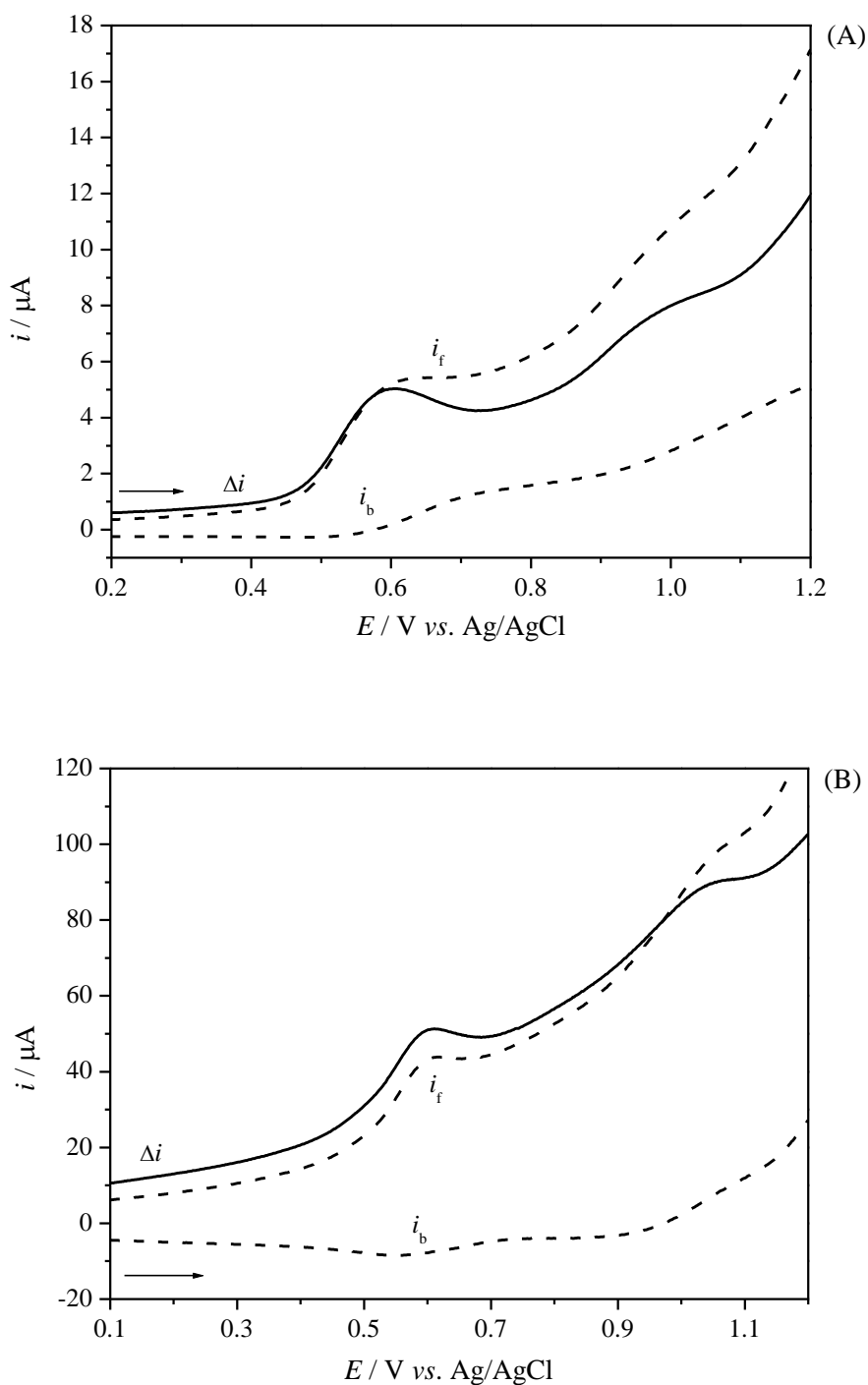


Figure 6. Square-wave voltammograms of 5×10^{-4} M K048 in 0.1 M KNO_3 at pH 9 for: (A) $f = 8$ Hz and (B) $f = 100$ Hz. The net response (Δi) and its forward (i_f) and backward (i_b) components are shown. The amplitude is 50 mV and the potential increment is 2 mV.

3.3 TMB-4

The cyclic voltammogram of 1×10^{-3} M TMB-4 recorded at scan rate of 25 mV s^{-1} , Fig. 7A, showed two consecutive charge transfer reactions, peak 1, at $E_1 = 0.627$ V, and peak 2, at $E_2 = 1.030$ V,

whereas CVs recorded at $\nu \geq 250 \text{ mV s}^{-1}$ (see Fig 7B) present only peak 1. On the negative going scan no peaks were obtained indicating irreversible electrooxidation of TMB-4. Analysis of the effect of scan rate on voltammograms showed that peak potentials of both peak 1 and peak 2 are shifted to the positive direction by increasing the scan rate.

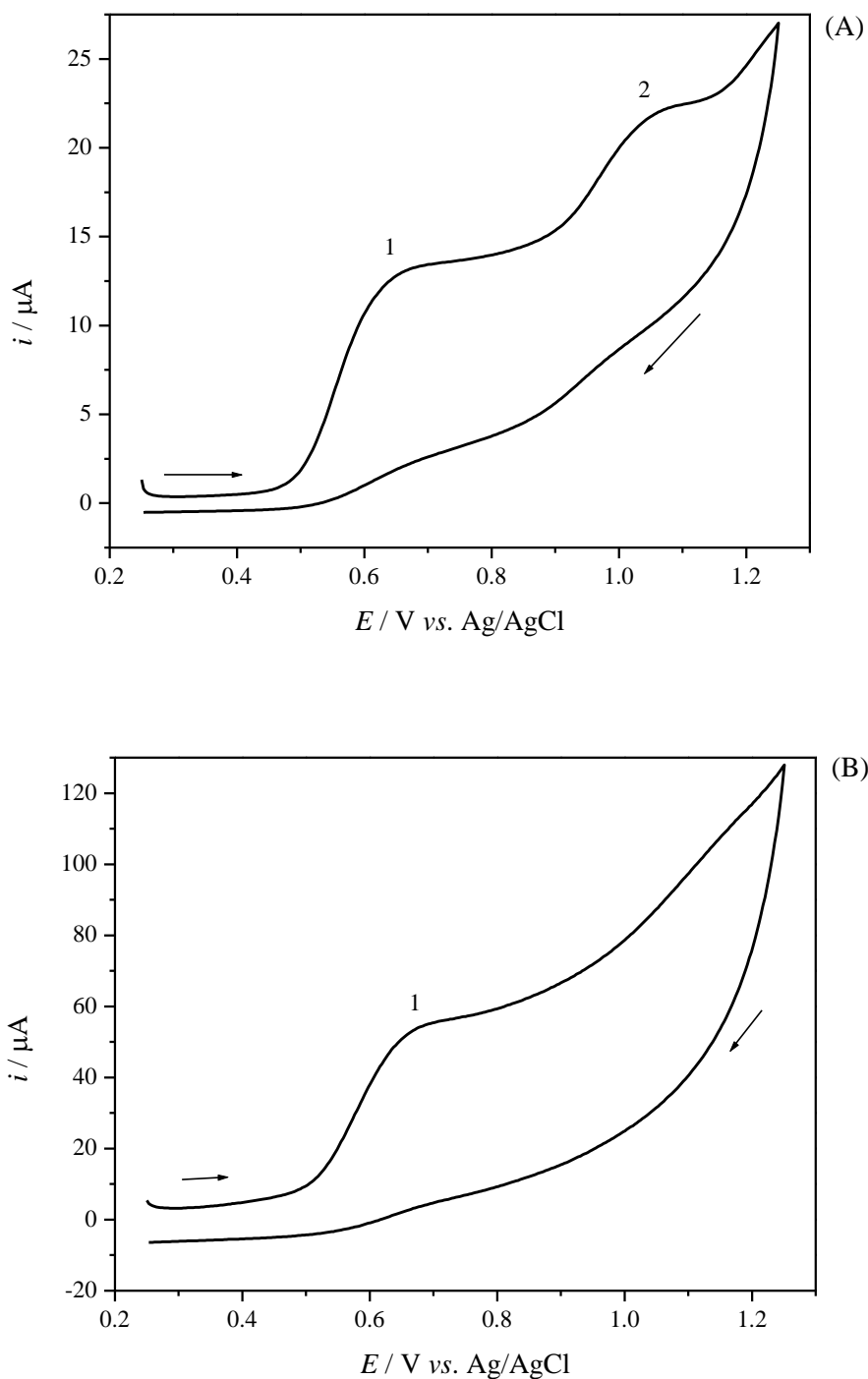


Figure 7. Cyclic voltammograms of $1 \times 10^{-3} \text{ M}$ TMB-4 in 0.1 M KNO_3 at pH 9: for (A) $\nu = 25 \text{ mV s}^{-1}$ and (B) $\nu = 500 \text{ mV s}^{-1}$. The potential increment is 3 mV .

Fig. 8 shows examples of SW voltammograms of 5×10^{-4} M TMB-4 solution recorded at pH 8 and two different SW frequencies. If $f = 8$ Hz, SW response consists of two peaks, peak 1, at 0.605 V, and peak 2, at 0.972 V. On the backward scan, only one reduction peak occurred, at 0.895 V. This peak corresponds to the reduction of products formed during the second electrode reaction. At $f = 50$ Hz, a new reduction peak at 0.565 V appears, and the second SW response completely disappears.

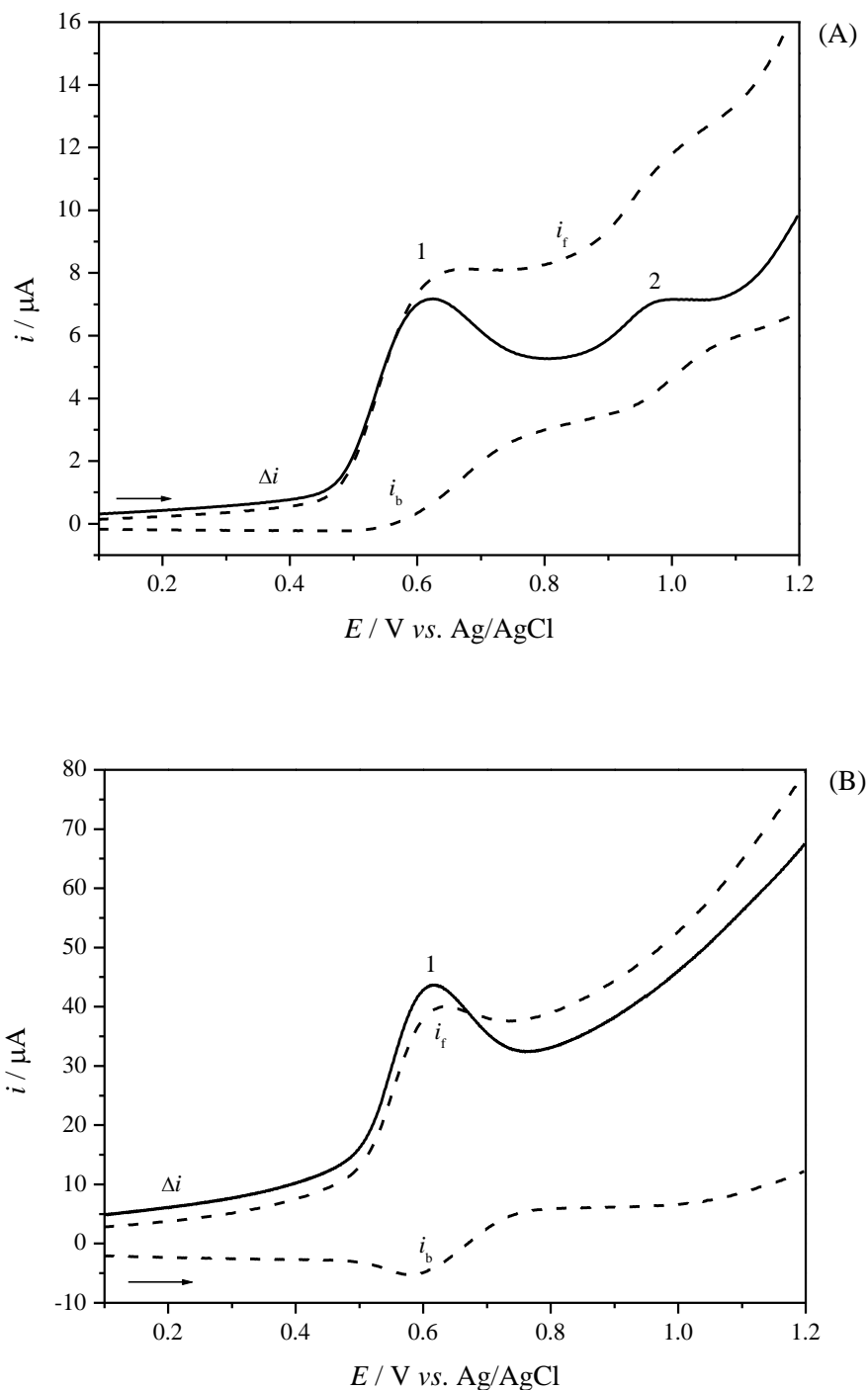


Figure 8. Square-wave voltammograms of 5×10^{-4} M TMB-4 in 0.1 M KNO_3 at pH 8 for: (A) $f = 8$ Hz and (B) $f = 100$ Hz. The net response (Δi) and its forward (i_f) and backward (i_b) components are shown. The amplitude is 50 mV and the potential increment is 2 mV.

The net peak current and the backward current of the first SW response increase by increasing frequency. Such behaviour is indicative of EC mechanisms [33]. Linear dependence of the net peak current of peak 1 on the square root of frequency indicates a diffusion controlled process. In the frequency range from 8 to 500 Hz, the peak 1 potential remains almost constant.

The experiments showed that the SW response of TMB-4 depends on pH of the medium. The pH study of TMB-4 oxidation was performed in a 5×10^{-4} M TMB-4 solution in a pH range from 3 to 11, and at frequency of 100 Hz. Below pH 5 no response can be recorded. In the range between pH 5 and pH 8, SW response showed a single oxidation peak, see Fig. 8B, which can be ascribed to the oxidation of oxime group. At $\text{pH} \geq 9$ a new broad and ill-defined peak 2 appears at more positive potentials (Fig. 9). For example, if $\text{pH} = 10$, peak 2 is shifted about 400 mV more positively with regard to peak 1. Similar voltammetric behaviour has been reported by Čakar et al. [33] for bis-imidazolium oximes. Namely, these authors claimed that, after the oxidation of one oxime group is finished, the second oxidation is shifted ca. 300 mV more positively. Moreover, they observed the second oxidation peak only at $\text{pHs} \geq \text{p}K_a(\text{—HC=NOH})$, indicating that deprotonation of the second oxime group undoubtedly precedes its oxidation. The second oxidation occurs at more positive potentials because of more difficult dissociation of the second oxime group. Taking into account the abovementioned data and considering that dissociation constant of the second oxime moiety in TMB-4 molecule is 9.5 [30], it can be concluded that peak 2 in Fig. 9 originates from the oxidation of this group.

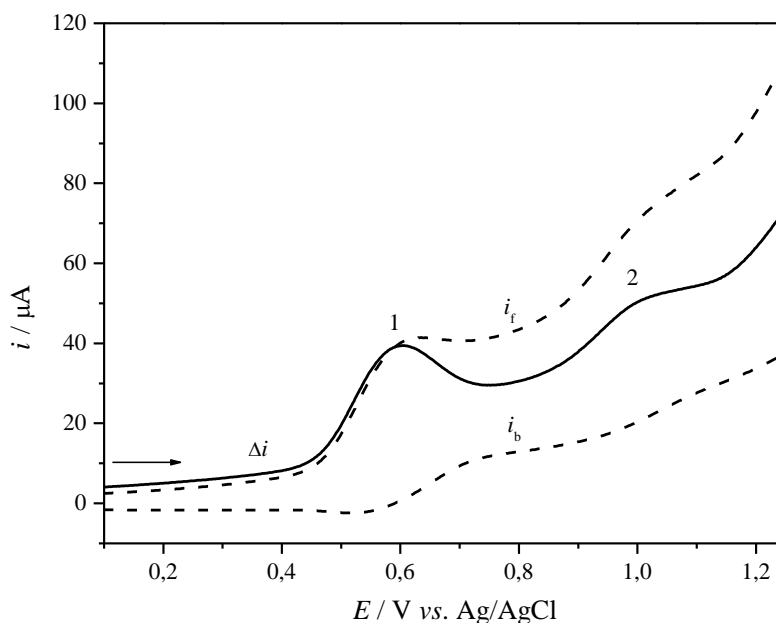


Figure 9. Square-wave voltammogram of 5×10^{-4} M TMB-4 in 0.1 M KNO_3 at pH 10. The net response (Δi) and its forward (i_f) and backward (i_b) components are shown. The frequency is 100 Hz, the amplitude is 50 mV and the potential increment is 2 mV.

As can be seen in Figs. 8B and 9, the product of the first electrode reaction can be electro-reduced back to the original molecule during the reverse half period of the SW signal, whatever the

pH. However, similarly to HI-6, the backward component decreases relative to the forward component by increasing the pH value indicating that the rate of the follow-up chemical reaction, by which the oxidation intermediate of TMB-4 is transformed, increases with increasing concentration of hydroxide ions in solution.

Fig. 10 shows the variation of potentials and currents of peak 1 with the solution pH. In the range between pH 5 and pH 8 the potential of peak 1 is a linear function of pH, with the slope -53 mV per pH unit. This slope value indicates a process that involves the same number of electrons and protons. For $\text{pH} > 8$, peak 1 potential is pH independent. Current maxima for peak 1 was observed at pH 8.

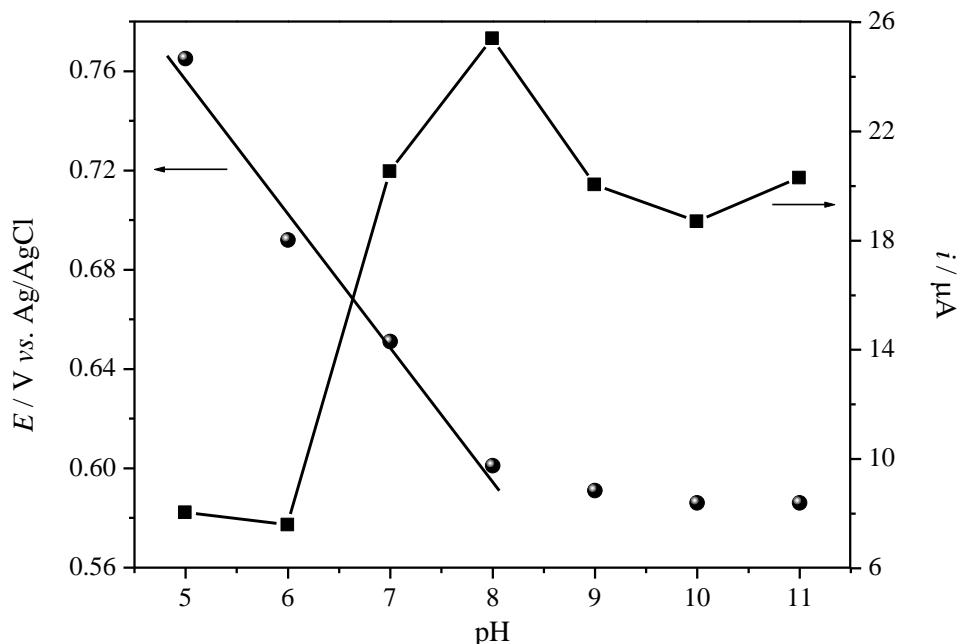


Figure 10. Dependence of net peak potentials (●) and net peak currents (▲) of the first electrode reaction of TMB-4 on pH of electrolyte. All other data are as in Fig. 9.

The influence of concentration on voltammetric response of TMB-4 was studied using square-wave voltammetry at a frequency of 100 Hz and pH 9. Interestingly, the net peak potential of the first response is shifted toward more positive values by increasing the concentration of TMB-4, which was not the case for HI-6 and K048. The relationship between peak 1 potential and the logarithm of TMB-4 concentration is linear, with the slope of $\Delta E_1/\Delta \log c = 28$ mV/d.u. Such behaviour is known for electrode reactions followed by the dimerization of product [34, 35].

The abovementioned experimental results indicate that the oxidation of TMB-4 proceeds via one or two consecutive reactions, depending on the pH. In the pH range between 5 and 8, TMB-4 exhibited only one anodic peak, corresponding to the oxidation of oxime group to hydroxy-nitroso intermediate via two-electrons two-protons ECE mechanism, as described by the reactions given in Scheme 2. Final product of this electrode reaction, hydroxy-nitroso intermediate, undergoes dimerization reactions, followed by decomposition to give a carbonyl compound and hyponitrous acid [25, 29, 36]. It is worth noting the difference in electrooxidation mechanisms (regarding the number of

protons involved) between TMB-4 and two other oximes studied here: two protons are involved in mechanism of electrooxidation of TMB-4, and only one proton participates in electrooxidation of HI-6 and K048. In the case of HI-6 and K048, deprotonation of oxime group occurs fast and is not the rate determining step. However, proton concentration does determinate the rate of chemical reaction that follows the first electron transfer, and we have shown that the number of protons involved in this step is 1 proton per molecule. As for TMB-4, the deprotonation of oxime group appears to be much more demanding, as the consequence of certain steric effects [30]. So, the deprotonation of oxime group (i.e. the first step of the reaction mechanism shown in Scheme 2) is a slow and rate-determining step for the reaction of electrochemical oxidation of oxime moiety to iminoxy radical. Furthermore, proton concentration in the electrolyte solution affects the rate of the second electron-transfer step as well, i.e. electro-oxidation of iminoxy radical to hydroxy-nitroso intermediate. If $\text{pH} \geq 9$, peak 2 occurred due to oxidation of the second oxime group in TMB-4 molecule. We assume that the oxidation mechanism of this group follows the same route as that proposed in Scheme 2. However, presently available data are insufficient to reliably elucidate the mechanism.

4. CONCLUSIONS

The results of this study have shown that the electrochemical oxidation of oximes (HI-6, K048 and TMB-4) on a glassy-carbon electrode, which corresponds to oxidation of oxime moiety, is diffusion controlled, pH dependent process that occurs in a complex ECE mechanism. The first step involves the oxidation of oxime moiety with formation of iminoxy radical that undergoes nucleophilic attack by water to give hydroxy-nitroso intermediate. The rate of chemical transformation of iminoxy radical is controlled by the proton concentration. The final product of this ECE reaction (i.e. the hydroxy-nitroso intermediate) undergoes slow oxidation at more positive potential. Unlike monoximes (HI-6 and K048), that exhibited only one anodic peak, TMB-4 undergoes two consecutive oxidation reactions due to the presence of two oxidizable oxime moieties. The first electrode reaction follows the abovementioned ECE mechanism. The second electro-oxidation reaction of TMB-4, is shifted around 400 mV more positively with regard to the first oxidation, and is possible only if $\text{pH} \geq 9$.

ACKNOWLEDGEMENT

Financial support from the Croatian Ministry of Science, Education and Sport, Project Numbers 022-0222148-2142, 098-0982904-2907 and 022-0222148-2139, is gratefully acknowledged. Also, authors would like to thank to Dr. Kamil Kuča (Faculty of Military Health Sciences, Hradec Králové, Czech Republic) for preparing and supplying the oximes HI-6 and K048.

References

1. R. M. Dawson, *J. Appl. Toxicol.*, 14 (1994) 317.
2. B. Antonijević, M. P. Stojiljković, *Clin. Med. Res.*, 5 (2007) 71.
3. E. Reiner, *Arh. Hig. Rada Toksikol.*, 52 (2001) 323.
4. F. Terrier, P. Rodriguez-Dafonte, E. Le Gueval, G. Moutiers, *Org. Biomol. Chem.*, 4 (2006) 4352.
5. M. P. Stojiljković, M. Jokanović, *Arh. Hig. Rada Toksikol.*, 57 (2006) 435.

6. K. Kuča, K. Musilek, D. Jun, J. Bajgar, J. Kassa, in *Handbook of toxicology of chemical warfare agents*, Elsevier Inc., Oxford (2009).
7. M. Čalić, A. Lucić Vrdoljak, B. Radić, D. Jelić, D. Jun, K. Kuča, Z. Kovarik, *Toxicology*, 219 (2006) 85.
8. S. Berend, A. Lucić Vrdoljak, B. Radić, K. Kuča, *Chem. Biol. Interact.*, 175 (2008) 413.
9. Z. Kovarik, A. Lucić Vrdoljak, S. Berend, M. Katalinić, K. Kuča, K. Musilek, B. Radić, *Arh. Hig. Rada. Toksikol.*, 60 (2009) 19.
10. N. J. Park, Y. S. Jung, K. Musilek, D. Jun, K. Kuča, *Bull. Korean. Chem. Soc.*, 27 (2006) 1401.
11. K. Kuča, K. Musilek, D. Jun, M. Pohanka, K. Kumar Ghosh, M. Hrabínova, *J. Enzyme Inhib. Med. Chem.*, 25 (2010) 509.
12. J. P. Ley, H. J. Bertram, *Eur. J. Lipid Sci. Technol.*, 104 (2002) 319.
13. G. O. Puntel, P. Gubert, G. L. Peres, L. Bresolin, J. B. T. Rocha, M. E. Pereira, V. S. Carratu, F. A. Antunes Soares, *Mol. Toxicol.*, 82 (2008) 755.
14. G. O. Puntel, N. R. de Carvalho, P. Gubert, A. S. Palma, C. Lenz Dalla Corte, D. Silva Avila, M. E. Pereira, V. S. Carratu, L. Bresolin, J. B. Teixeira da Rocha, F. A. Antunes Soares, *Chem. Biol. Interact.*, 177 (2009) 153.
15. T. Özen, M. Taş, *J. Enzyme Inhib. Med. Chem.*, 24 (2009) 1141.
16. P. Kovačić, *Curr. Med. Chem.*, 10 (2003) 2705.
17. B. Radić, A. Lucić Vrdoljak, D. Želježić, N. Fuchs, S. Berend, N. Kopjar, *Acta Biochim. Polon.*, 54 (2007) 583.
18. A. P. da Silva, M. Farina, J. L. Franco, A. L. Dafre, J. Kassa, K. Kuča, *Neurotoxicology*, 29 (2008) 184.
19. M. Pohanka, J. Zdarova Karasova, K. Musilek, K. Kuča, Y. S. Jung, J. Kassa, *J. Enz. Inhib. Med. Chem.*, 26 (2011) 93.
20. A. Antunes dos Santos, D. Bonfanti dos Santos, R. Pietsch Ribeiro, D. Colle, K. C. Peres, J. Hermes, A. Machado Barbosa, A. L. Dafré, A. F. de Bem, K. Kuča, M. Farina, *NeuroToxicology*, 32 (2011) 888.
21. D. M. Frank, P. K. Arora, J. L. Blumer, L. M. Sayre, *Biochem. Biophys. Res. Commun.*, 147 (1987) 1095.
22. A. J. Roman, J. M. Sevilla, T. Pineda, M. Blazquez, *J. Electroanal. Chem.*, 410 (1996) 15.
23. A. J. Roman, J. M. Sevilla, T. Pineda, M. Blazquez, *J. Electroanal. Chem.*, 485 (2000) 1.
24. Š. Komorsky-Lovrić, *J. Electroanal. Chem.*, 289 (1990) 161.
25. S. Issac, K. G. Kumar, *Anal. Methods*, 2 (2010) 1484.
26. M. Lovrić, Š. Komorsky-Lovrić, *Int. J. Electrochem.*, 2012 (2012) 305.
27. V. Mirčeski, M. Lovrić, *Croat. Chem. Acta*, 73 (2000) 305.
28. R. C. Reed, M. Wightman, in *Encyclopedia of Electrochemistry of Elements*, Vol. XV, Marcel Dekker, New York (1984).
29. L. Bencharif, A. Tallec, R. Tardivel, *Electrochim. Acta*, 42 (1997) 3509.
30. G. Šinko, M. Čalić, Z. Kovarik, *FEBS Lett.*, 580 (2006) 3167.
31. H. C. Kim, M. Mickel, N. Hampp, *Chem. Phys. Lett.*, 371 (2003) 410.
32. V. Mirčeski, Š. Komorsky-Lovrić, M. Lovrić, *Square-Wave voltammetry*, Springer, Berlin (2007).
33. M. M. Čakar, V. M. Vasić, Lj. T. Petkovska, D. Lj. Stojić, M. Amramov-Ivić, G. A. Milovanović, *J. Pharm. Biomed. Anal.*, 20 (1999) 655.
34. M. Lovrić, D. Jadreško, Š. Komorsky-Lovrić, *Electrochim. Acta*, 90 (2013) 226.
35. R. Meunier- Prest, C. Gaspard, E. Laviron, *J. Electroanal. Chem.*, 410 (1996) 145.
36. J. W. Bird, D. G. M: Diaper, *Can. J. Chem.*, 47 (1969) 145.